PHYSICAL REVIEW D **92,** 054011 (2015)

States generated in the K–multi-ρ interactions

C. W. Xiao

Institute for Advanced Simulation and Institut für Kernphysik (Theorie), Forschungszentrum Jülich, D-52425 Jülich, Germany
and Departamento de Física Teórica and IFIC, Centro Mixto Universidad de Valencia-CSIC, Institutos de Investigación de Paterna, Apartado 22085, 46071 Valencia, Spain

(Received 6 February 2015; published 9 September 2015)

In the present work, we use three-body interaction formalism to investigate the K–multi-ρ interactions. First, we reproduce the resonances $f_2(1270)$ and $K_1(1270)$ in the $\rho\rho$ and ρK two-body interactions, respectively, as the clusters of the fixed-center approximation. Then, we study the three-body K–$\rho\rho(f_2)$ and ρ–$\rho K(K_1)$ interactions with the fixed-center approximation of the Faddeev equations. Furthermore, we extrapolate the formalism to study the four-body, five-body, and six-body systems containing one K meson and multiple ρ mesons. In our research, without introducing any free parameters, we generate the $K_2(1770)$ state in the three-body interaction with the mass of 1707 MeV and a width about 113 MeV, which are consistent with the experiments. We also find a clear resonant structure in our results of the five-body interaction, with a mass 2505 MeV and a width about 32 MeV or more, which is associated with the $K_4(2500)$ state, where we obtain consistent results with the experimental findings. Furthermore, we predict some new states in the other many-body interactions, $K_3(2080)$, $K_5(2670)$ (isospin $I = 1/2$), and $K_4(2640)$ (isospin $I = 3/2$), with uncertainties.

DOI: 10.1103/PhysRevD.92.054011 PACS numbers: 11.80.Jy, 12.38.Lg, 12.39.Fe, 13.75.Lb

I. INTRODUCTION

To understand the nature and structure of the particles found in experiments and to search for new hadronic states are the main issues in present-day particle physics, which has generally accepted that quarks are the basic building blocks of matter. Within the Gell-Mann-Zweig quark model [1,2] for the normal hadron states, mesons are made of a quark-antiquark pair, $q\bar{q}$, and baryons are made of three quark components, qqq. On the other hand, there are some states found in the experiments, such as the mesons $f_0(500)$, $f_0(980)$, $a_0(980)$, $\kappa(800)$, and the baryons $\Lambda(1405)$, $N(1440)$, $N(1535)$, with structure and properties difficult to explain by the normal quark model. These states might therefore be called "exotic" states (recent experimental discussions are given in Refs. [3,4]). To understand the structure and properties of these exotic states in the strong interaction, we need to exploit other theories or approaches, for example chiral perturbative theory [5–11], effective field theory [12–14], lattice QCD [15–17], the QCD sum rule [18–21], Dyson-Schwinger equations [22–24], the chiral quark model [25–27], the chiral unitary approach (ChUA) [28–33], and so on. But some discovered particles, such as the $\phi(2170)$ [also called $X(2175)$ or $Y(2175)$], the $Y(4260)$, and the $N^*(1710)$, appear to have a more complicated structure and could come from multibody hadron interaction, which is a subject in hadron physics that has drawn much attention for a long time [34–38]. With this motivation, the work of Ref. [39] develops the ChUA for the three-body interaction, which combines the three-body Faddeev equations with an on-shell approximation of the ChUA and has reported several S-wave $J^P = \frac{1}{2}^+$ resonances qualifying as two meson–one baryon molecular states. In Ref. [40], this combination of Faddeev equations and chiral dynamics in the $DK\bar{K}$ system obtains consistent results with QCD sum rules. When in some cases there are resonances (or bound states) appearing in the two-body subsystem of the three-body interaction, Ref. [41] takes the fixed-center approximation (FCA) [35,42–46] to the Faddeev equations, where several multi-$\rho(770)$ states are dynamically produced, and the resonances $f_2(1270)(2^{++})$, $\rho_3(1690)(3^{--})$, $f_4(2050)(4^{++})$, $\rho_5(2350)(5^{--})$, and $f_6(2510)(6^{++})$ are theoretically found as basically molecules of an increasing number of $\rho(770)$ particles with parallel spins. Analogously, the resonances $K_2^*(1430)$, $K_3^*(1780)$, $K_4^*(2045)$, $K_5^*(2380)$, and a new K_6^* are produced in the K^*–multi-ρ systems and could be explained as molecules with the components of an increasing number of $\rho(770)$ and one $K^*(892)$ meson in Ref. [47]. Also, in Ref. [48], charmed resonances D_3^*, D_4^*, D_5^*, and D_6^* are predicted in the D^*–multi-ρ interaction. Note that recently a resonance structure was found by LHCb at about 2.8 GeV with $J^P = 3^-$ in the $\bar{D}^0\pi^-$ mass distribution [49], which is close to the mass of the D_3^* state predicted in Ref. [48], 2800–2850 MeV. In the present work, we investigate the K–multi-ρ interaction.

Taking FCA to the Faddeev equations, the $\bar{K}NN$ interaction studied in Refs. [50,51] has proven accurate when dealing with bound states, and obtains consistent results with the full Faddeev equations evaluation without taking FCA [52] or a variational calculation with a non-relativistic three-body potential model [53], which is also confirmed by the recent results with new Faddeev

calculations in Refs. [54,55]. Even though there is a different result claimed in Ref. [56] on the $\bar{K}NN$ system, the work of Ref. [57] clarified the different kinematical properties between them using two different approaches in their investigations, the Watson approach and the truncated Faddeev approach. A further study of the $\bar{K}NN$ system is done in the recent work of Ref. [58], which has investigated the $\bar{K}d$ scattering length with the first-order recoil correction using the nonrelativistic effective field theory approach. A narrow quasibound state of 3500 MeV in the DNN system is predicted in Ref. [59] by both the FCA to Faddeev equations calculation and the variational method approach with the effective one-channel Hamiltonian. Therefore, in the present work, we use the FCA to the Faddeev equations to investigate the K–multi-ρ interaction. There are some possible K excited states with strangeness $S = \pm 1$ and aligned with increasing spin number in the Particle Data Group (PDG) findings [60], such as $K_1(1270)(1^+)$ or $K_1(1400)(1^+)$ or $K_1(1650)(1^+)$, $K_2(1580)(2^-)$ or $K_2(1770)(2^-)$ or $K_2(1820)(2^-)$ or $K_2(2250)(2^-)$, $K_3(2320)(3^+)$, and $K_4(2500)(4^-)$. Some of these states still need more confirmation in future experiments. This is the motivation of the present work, to understand their structure and properties theoretically. Applying the FCA to the Faddeev equations, there should be resonances or bound states in the two-body subsystem. For the K–multi-ρ systems, the basic two-body subsystems are the $\rho\rho$ and $K\rho$ interactions. Based on the local hidden gauge Lagrangians [61–64], the two-body $\rho\rho$ interaction is studied in Ref. [65] with the coupled channel approach of ChUA, and it is found that a $\rho\rho$ quasibound state or molecule could be associated with the $f_2(1270)$ found in the PDG data [60]. With the on-shell Bethe-Salpeter equation of ChUA and a chiral Lagrangian, the two-body $K\rho$ interaction is studied in Ref. [66] and dynamically produces the $K_1(1270)$ resonance. Furthermore, the $K_1(1270)$ state is reinvestigated with detail using ChUA to analyze the experimental data in the later work of Ref. [67]. Thus, the resonances $f_2(1270)$ in the $\rho\rho$ interaction and $K_1(1270)$ in the $K\rho$ interaction are the needed clusters in the formalism of the present work.

In the next section, we will first present the formalism of the FCA to the Faddeev equations. Then, in the following section, the resonances $f_2(1270)$ and $K_1(1270)$ are reproduced dynamically with the ChUA in the $\rho\rho$ interaction and in the $K\rho$ interaction, respectively. Our investigation results are shown in Sec. IV. Finally, we present our conclusions.

II. FORMALISM

For the three-body interaction, as Faddeev suggested in Ref. [35], the scattering amplitude of the T matrix can be written as a sum of three partitions,

$$T = T^1 + T^2 + T^3, \tag{1}$$

where partition amplitude T^i ($i = 1, 2, 3$) includes all the possible interactions contributing to the three-body T matrix, with the particle i being a spectator in the last interaction. But if there are resonances (or bound states) as clusters appearing in the two-body subsystem interaction, for example the cluster coming from T^3, we can assume that a cluster is formed by the two particles (named particles 1 and 2) and is not much modified by the interaction of a third particle (particle 3) with this cluster. Therefore, assuming the cluster as the fixed center of the three-body system, we can take the FCA [35,42–46] to the Faddeev equations. Then, the T^3 partition amplitude contributes to the cluster for the FCA, and the FCA multiple scattering of the third particle with the components of the cluster is taken into account. Thus, we can rewrite the Faddeev equations of Eq. (1) easily (which is also developed by the ChUA):

$$T_1 = t_1 + t_1 G_0 T_2, \tag{2}$$

$$T_2 = t_2 + t_2 G_0 T_1, \tag{3}$$

$$T = T_1 + T_2, \tag{4}$$

where T is the total three-body scattering amplitude, as depicted in Fig. 1. From this figure, we can see that the Faddeev equations under the FCA are first a pair of particles (1 and 2) forming a cluster, and then particle 3 interacts with the components of the cluster, undergoing all possible multiple scattering with those components. Thus, the two partition amplitudes T_1 and T_2 sum all diagrams of the series of Fig. 1 which begin with the interaction of particle 3 with particle 1 of the cluster (T_1), or with the particle 2 (T_2). Finally, the scattering amplitude T is the total three-body interaction amplitude that we look for. The amplitudes t_1 and t_2 represent the unitary scattering amplitudes with coupled channels for the interactions of particle 3 with particles 1 and 2, respectively, which should be taken into account in the isospin structure of the subsystem and is discussed in detail for different cases in Sec. IV. Besides this, G_0 is the propagator of particle 3 between the components of the two-body subsystem, given by

$$G_0(s) = \frac{1}{2M_R} \int \frac{d^3\vec{q}}{(2\pi)^3} F_R(\vec{q}) \frac{1}{q^{02}(s) - \vec{q}^2 - m_3^2 + i\epsilon}, \tag{5}$$

where $q^0(s)$, the energy carried by particle 3 in the rest frame of the three-particle system, is given by

$$q^0(s) = \frac{s + m_3^2 - M_R^2}{2\sqrt{s}}, \tag{6}$$

with m_3 being the mass of the third particle and M_R the mass of the cluster, and $F_R(\vec{q})$ is the form factor of the cluster of particles 1 and 2. The form factor of the cluster should be consistent with the theory used to generate the cluster.

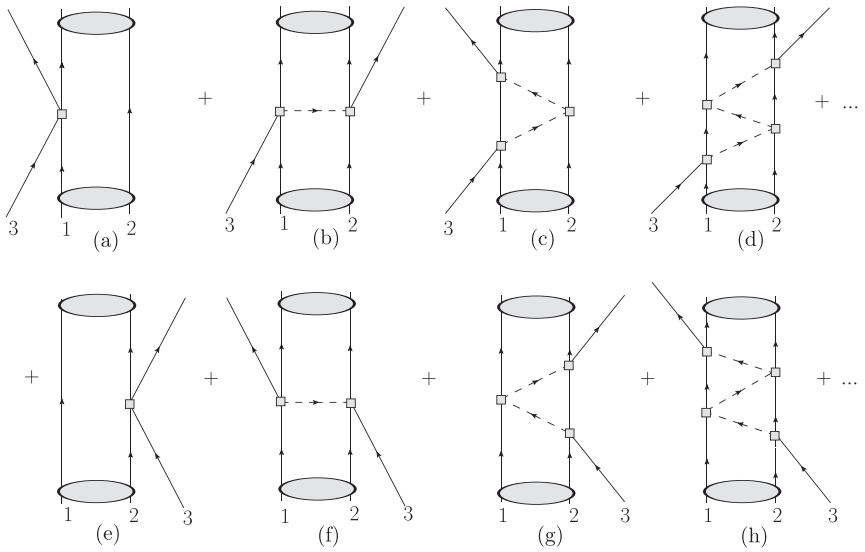

FIG. 1. Diagrammatic representation of the FCA to Faddeev equations: (a) and (e) are the single scattering, (b) and (f) the double-scattering, and so on.

This requires us to evaluate the wave functions in the ChUA reproduced in the cluster, which has been done in Refs. [68–70] for S-wave bound states, S-wave resonant states, and states with arbitrary angular momentum, respectively. Since in the present cases, the generated clusters are S-wave bound states, we only need the expression of the form factors for the S-wave bound states, given by [69]

$$F_R(\vec{q}) = \frac{1}{\mathcal{N}} \int_{|\vec{p}|<\Lambda', |\vec{p}-\vec{q}|<\Lambda'} d^3\vec{p} \frac{1}{2\omega_1(\vec{p})} \frac{1}{2\omega_2(\vec{p})} \frac{1}{M_R - \omega_1(\vec{p}) - \omega_2(\vec{p})} \frac{1}{2\omega_1(\vec{p}-\vec{q})} \frac{1}{2\omega_2(\vec{p}-\vec{q})} \frac{1}{M_R - \omega_1(\vec{p}-\vec{q}) - \omega_2(\vec{p}-\vec{q})}, \tag{7}$$

$$\mathcal{N} = \int_{|\vec{p}|<\Lambda'} d^3\vec{p} \left(\frac{1}{2\omega_1(\vec{p})} \frac{1}{2\omega_2(\vec{p})} \frac{1}{M_R - \omega_1(\vec{p}) - \omega_2(\vec{p})}\right)^2, \tag{8}$$

where $\omega_i = \sqrt{\vec{q}^2 + m_i^2}$ ($i = 1, 2$, m_i the mass) are the energies of the particles 1 and 2. We use a cutoff Λ' to regularize the integrals of Eqs. (7) and (8) [also for Eq. (5), discussed in Sec. IV], which is the same as the one used in the loop function of the two-body interaction to reproduce the cluster [47,71]. Thus, no free parameters are involved. Note that, in the present work, we care about the dynamics close to the threshold, and thus the method of cutoff is acceptable.[1]

Taking the normalization of the field theory [74] which has different weight factors for the particle fields, we must take into account how these factors appear in the single scattering and double scattering and in the total amplitude [47,71]. In all the present cases, the cluster (also particles 1 and 2) is a meson, and the scattering particle (the third particle) is too, which means they are only related to meson fields. Thus, following Ref. [74], we write the S matrix of single scattering, Figs. 1(a) and (e):

$$S_1^{(1)} = -it_1(2\pi)^4\delta(k + k_R - k' - k'_R) \times \frac{1}{\mathcal{V}^2} \frac{1}{\sqrt{2\omega_3}} \frac{1}{\sqrt{2\omega'_3}} \frac{1}{\sqrt{2\omega_1}} \frac{1}{\sqrt{2\omega'_1}}, \tag{9}$$

$$S_2^{(1)} = -it_2(2\pi)^4\delta(k + k_R - k' - k'_R) \times \frac{1}{\mathcal{V}^2} \frac{1}{\sqrt{2\omega_3}} \frac{1}{\sqrt{2\omega'_3}} \frac{1}{\sqrt{2\omega_2}} \frac{1}{\sqrt{2\omega'_2}}, \tag{10}$$

where, k, k' (k_R, k'_R) are the momenta of the initial and final scattering particles (R for the cluster); ω_i, ω'_i are the energies of the initial and final particles; $\mathcal{V}$ is the volume of the box where the states are normalized to unity; and the subscripts 1, 2 refer to scattering with particle 1 or 2 of the cluster.

Next, the double-scattering diagrams, Figs. 1(b) and (f), are given by

[1]We use a common cutoff method to regularize the propagator. Since it violates gauge invariance, it is a effective way to remove infinities from perturbative calculations, of which the problem is addressed in Ref. [72] within the effective Lagrangian. Furthermore, respecting Lorentz invariance, the cutoff regularization can recover the symmetry [73] (references therein).

$$S^{(2)} = -i(2\pi)^4\delta(k+k_R-k'-k'_R)\frac{1}{\mathcal{V}^2}\frac{1}{\sqrt{2\omega_3}}\frac{1}{\sqrt{2\omega'_3}}\frac{1}{\sqrt{2\omega_1}} \times \frac{1}{\sqrt{2\omega'_1}}\frac{1}{\sqrt{2\omega_2}}\frac{1}{\sqrt{2\omega'_2}}\int\frac{d^3q}{(2\pi)^3}F_R(\vec{q}) \times \frac{1}{q^{02}-\vec{q}^2-m_3^2+i\epsilon}t_1t_2, \quad (11)$$

where $F_R(\vec{q})$ is the cluster form factor that we have discussed above, seen in Eq. (7).

Similarly, the full S matrix for scattering of particle 3 with the cluster can be written as

$$S = -iT(2\pi)^4\delta(k+k_R-k'-k'_R) \times \frac{1}{\mathcal{V}^2}\frac{1}{\sqrt{2\omega_3}}\frac{1}{\sqrt{2\omega'_3}}\frac{1}{\sqrt{2\omega_R}}\frac{1}{\sqrt{2\omega'_R}}. \quad (12)$$

Now, we can see that for the unitary amplitudes corresponding to the single-scattering contribution, one must take into account the isospin structure of the cluster and write the t_1 and t_2 amplitudes in terms of the isospin amplitudes of the (3, 1) and (3, 2) systems. In view of the different normalization of these terms by comparing Eqs. (9), (10), (11), and (12), we can introduce suitable factors in the elementary amplitudes,

$$\tilde{t_1} = \frac{2M_R}{2m_1}t_1, \qquad \tilde{t_2} = \frac{2M_R}{2m_2}t_2, \quad (13)$$

where we have taken the approximations $\frac{1}{\sqrt{2\omega_i}} \simeq \frac{1}{\sqrt{2m_i}}$. But when the cluster—the particles 1 and 2—includes a baryon, the factors in Eqs. (5) and (13), $2M_R$ and $2m_i$, should be replaced by 1 for taking the baryonic field factor approximation $\sqrt{\frac{2M_B}{2E_B}} \approx 1$. Finally, we sum all the diagrams, obtaining

$$T = T_1 + T_2 = \frac{\tilde{t_1}+\tilde{t_2}+2\tilde{t_1}\,\tilde{t_2}\,G_0}{1-\tilde{t_1}\,\tilde{t_2}\,G_0^2}. \quad (14)$$

When $\tilde{t_1} = \tilde{t_2}$ in some cases, it can be simplified as

$$T = \frac{2\tilde{t_1}}{1-\tilde{t_1}G_0}. \quad (15)$$

Note that the FCA to Faddeev equations calculation is particularly suited to study a system with the subsystem bound or even loose bound, as discussed in Refs. [50,51], and has some limitation on the case when the cluster of the two particles in the subsystem is excited in the intermediate states (more discussions can be seen in Ref. [75] for the study of a $\phi K\bar{K}$ system).

From the S matrix of single scattering, Eqs. (9), (10), and the full S matrix, Eq. (12), we should note that the arguments of the amplitudes $T_i(s)$ and $t_i(s_i)$ are different, where s is the total invariant mass of the three-body system, and s_i are the invariant masses in the two-body subsystems. The relationship between them is given by [47]

$$s_i = m_3^2 + m_i^2 + \frac{(M_R^2+m_i^2-m_j^2)(s-m_3^2-M_R^2)}{2M_R^2}, \quad (i,j=1,2,i\neq j). \quad (16)$$

III. TWO-BODY INTERACTION

Using the Faddeev equations under the FCA, we first need bound states in the two-body subsystem as the cluster of the fixed center, and then let the third particle collide with the cluster and interact with the components of the forming cluster. As discussed in the Introduction, for the subsystems of the K–multi-ρ system, the two-body $\rho\rho$ and ρK interactions are studied in Refs. [65] and [67]. We briefly summarize their work to reproduce the resonances $f_2(1270)$ and $K_1(1270)$, and obtain the two-body scattering amplitudes of the subsystem (details given in the appendixes).

A. $\rho\rho$ interaction

In Ref. [65], the $\rho\rho$ interaction is studied with the local hidden gauge formalism [61–64] and the ChUA with coupled channels, and the $f_2(1270)$ $[I(J^{PC}) = 0(2^{++})]$ state is dynamically produced. From the local hidden gauge Lagrangians, the s-wave potentials of spin $S = 2$ for $\rho\rho$ interaction are obtained in the sectors of isospin $I = 0$ and $I = 2$:

$$V_{\rho\rho}^{(I=0,S=2)}(s_i) = -4g^2 - 8g^2\left(\frac{3s_i}{4m_\rho^2}-1\right), \quad (17)$$

$$V_{\rho\rho}^{(I=2,S=2)}(s_i) = 2g^2 + 4g^2\left(\frac{3s_i}{4m_\rho^2}-1\right), \quad (18)$$

where $g = M_V/2f_\pi$, with M_V being the vector meson mass and f_π the pion decay constant. The scattering amplitude of $\rho\rho$ interaction is calculated by the on-shell Bethe-Salpeter equation,

$$t^I = [1-V^IG^I]^{-1}V^I, \quad (19)$$

where the kernel V^I is a matrix of the interaction potentials, and G^I is a diagonal matrix of the loop functions (the upper index I represents the specific isospin sector).

Following the work of Ref. [65] (for more details, see Appendix A), we also take into account the contribution of the box diagram with two pseudoscalar mesons in the intermediate state. We only consider the imaginary part of the box diagram contribution as the correction of the potential V^I and neglect its real part, which is very small. Note that we do not take these intermediate channels in the box diagram (more detail seen in Ref. [65]) as accounting for the coupled channels [76,77]. On the other hand, as is done in Ref. [65], we also consider the ρ mass distribution by replacing the loop function in the corresponding channel with its convoluted form. We obtain consistent results with

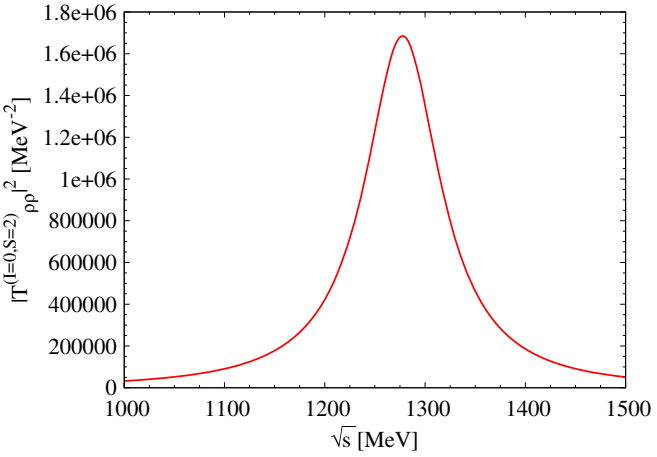

FIG. 2 (color online). Modulus squared of the scattering amplitudes: $|t^{I=0}_{\rho\rho}|^2$, with $f_2(1270)$ showing up.

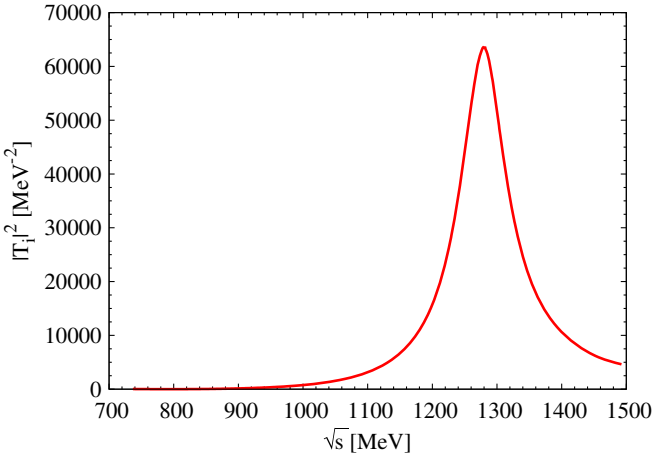

FIG. 3 (color online). Modulus squared of the scattering amplitudes: $|t^{I=1/2}_{\rho K}|^2$, with $K_1(1270)$ showing up.

Ref. [65], as shown in Fig. 2, where the structure of the resonance $f_2(1270)$ is found in the peak of the modulus squared of the amplitude. We have successfully reproduced the $f_2(1270)$ state as the cluster of our procedure. Besides, the nonresonant amplitude $t^{(I=2,S=2)}_{\rho\rho}$ is not shown in the figure, which is needed when we evaluate the two-body interaction amplitudes t_1, t_2, considering the isospin structure of the subsystem (discussed in Sec. IV).

B. ρK interaction

The ρK interaction is investigated by the ChUA in Refs. [66,67]. Following the work of Ref. [67], we can dynamically generate the $K_1(1270)$ resonance in the interaction of ρK and its couple channels, ϕK, ωK, $K^*\eta$, and $K^*\pi$. From the local hidden gauge Lagrangians, the vector-pseudoscalar potential projected over s-waves can be written as

$$V_{ij}(s_i) = -\frac{\vec{\epsilon}\cdot\vec{\epsilon}\,'}{8f^2}C_{ij}\Big[3s_i - (M_i^2 + m_i^2 + M_j^2 + m_j^2) - \frac{1}{s_i}(M_i^2 - m_i^2)(M_j^2 - m_j^2)\Big], \tag{20}$$

where $M_{i(j)}$ and $m_{i(j)}$ represent the masses of the $i(j)$ channel of the incoming (outgoing) particles, and the coefficients of C_{ij} can be found in Ref. [67] (also given in Appendix B). Then, we can input these potentials into the on-shell Bethe-Salpeter equation to evaluate the scattering amplitude,

$$t^I = [1 + V^I\hat{G}^I]^{-1}(-V^I)\vec{\epsilon}\cdot\vec{\epsilon}\,', \tag{21}$$

where $\hat{G}^I$ is $(1 + \frac{1}{3}\frac{q_l^2}{M_l^2})G^I$, being a diagonal matrix [with G^I as the normal loop function in Eq. (19)]; and $\vec{\epsilon}(\vec{\epsilon}\,')$ represents a polarization vector of the incoming (outgoing) vector meson. As is done in Ref. [67] (details of the convolution of G^I are given in Appendix C), we also take into account the large width of the vector mesons, and consider the convolution of the vector mesons as an intermediate state in the loop function G^I. In Fig. 3, we show our results for the modulus squared of $t^{I=1/2}_{\rho K}$, which are consistent with Ref. [67]. From the peak position, we can see that the $K_1(1270)$ is successfully reproduced in our work as the cluster in the FCA. In the $I = 3/2$ sector, there are only two coupled channels, ρK and $K^*\pi$, in which no resonance appeared. But for considering the isospin structure of the subsystem, we also evaluate the amplitude $t^{I=3/2}_{\rho K}$, which is not shown in the figure.

IV. RESULTS

In the present work, we study the K–multi-ρ interactions. In the former section, we have reproduced the resonances $f_2(1270)$ and $K_1(1270)$ in the $\rho\rho$ and ρK two-body interactions, which are the clusters of the FCA to Faddeev equations for the three-body interaction. Therefore, based on the possible clusters in the two-body interaction discussed above, the possible cases for the K–multi-ρ interactions are listed in Table I, and explained as follows. For the three-body interaction, we have two options: (i) particle $3 = K$, cluster or resonance $R = f_2$ (particle $1 = \rho, 2 = \rho$); and (ii) $3 = \rho$, $R = K_1$ $(1 = \rho, 2 = K)$. For the four-body interaction, we can extrapolate the FCA ideas and also have two cases: (i) $3 = f_2$, $R = K_1$ $(1 = \rho, 2 = K)$; and (ii) $3 = K_1$, $R = f_2$ $(1 = \rho, 2 = \rho)$. If we find a new resonance in the four-body interaction, assumed as K_3, there are also two cases for the five-body interaction: (i) $3 = K$, $R = f_4$ $(1 = f_2, 2 = f_2)$; and (ii) $3 = \rho$, $R = K_3$ $(1 = f_2, 2 = K_1)$. For the six-body interaction, (i) $3 = K_1$, $R = f_4$ $(1 = f_2, 2 = f_2)$; and (ii) $3 = f_2$, $R = K_3$ $(1 = f_2, 2 = K_1)$. We show our investigation results for all these cases below.

TABLE I. The cases considered in the K–multi-ρ interactions. Threshold 1: $m_3 + m_1 + m_2$; threshold 2: $m_3 + M_R$ (unit: MeV).

Particles:	3	R (1,2)	Amplitudes	Threshold 1	Threshold 2
Two-body	ρ	K	$t_{\rho K}$	1271.0	$(1270.0)_{K_1}$
	ρ	ρ	$t_{\rho\rho}$	1551.0	$(1275.1)_{f_2}$
Three-body	K	$f_2(\rho\rho)$	T_{K-f_2}	2046.5	1770.6
	ρ	$K_1(\rho K)$	$T_{\rho-K_1}$		2045.5
Four-body	K_1	$f_2(\rho\rho)$	$T_{K_1-f_2}$	2821.0	2545.1
	f_2	$K_1(\rho K)$	$T_{f_2-K_1}$	2546.1	
Five-body	K	$f_4(f_2f_2)$	T_{K-f_4}	3045.7	2513.5
	ρ	$K_3(f_2K_1)$	$T_{\rho-K_3}$	3320.6	(2855.5)
Six-body	K_1	$f_4(f_2f_2)$	$T_{K_1-f_4}$	3820.2	3288
	f_2	$K_3(f_2K_1)$	$T_{f_2-K_3}$		(3355.5)

A. Three-body interaction

In the three-body interaction, there are two possible structures: K–$f_2(\rho\rho)$ and ρ–$K_1(\rho K)$, which means that (i) $3 = K$, $R = f_2$ $(1 = \rho, 2 = \rho)$; and (ii) $3 = \rho$, $R = K_1$ $(1 = \rho, 2 = K)$. To evaluate these scattering amplitudes, we need as input the t_1 and t_2 amplitudes of the (3, 1) and (3, 2) subsystems, $t_1 = t_2 = t_{\rho K}$ for K–$f_2(\rho\rho)$ and $t_1 = t_{\rho\rho}, t_2 = t_{\rho K}$ for ρ–$K_1(\rho K)$. We can calculate them in the two-body $\rho\rho$ and ρK interactions, which are discussed in the previous section, following the work of Refs. [65,67]. But note that, in their work, the dimensional regularization scheme is used for the loop functions. To evaluate the form factor of the cluster, we need a cutoff Λ', which is the same as the one $q_{\max}$ used in the loop function for the two-body interaction, discussed in Sec. II. As discussed in Ref. [78], we can compare the value of the G function at threshold using the dimensional regularization formula [79] with that of the cutoff, which can be taken from Ref. [28] or the analytic expression in Ref. [80]. Then, equivalently to the parameters in the dimensional expression, we obtain $q_{\max} = 875$ MeV for the $f_2(1270)$ cluster and $q_{\max} = 1035$ MeV for the $K_1(1270)$ cluster. In fact, we do not introduce any free parameter.

With the values of these two $q_{\max}$ for the cutoff of Λ', then using Eqs. (7) and (8), we can evaluate the form factors of the clusters, $f_2(1270)$ and $K_1(1270)$, shown in Fig. 4 (left), where we can see that when $q \to 2\Lambda', F_R(q) \to 0$. Therefore, for the cutoff of the G_0 function, seen in Eq. (5), we choose as $2\Lambda'$ from the constraint of the form factor. Note that the form factor of Eq. (7) is only valid for the cluster of the bound state, which is the starting point of the FCA, since only the wave functions of the components of the bound state lead to the ordinary form factor, but not for the cluster of resonance [69] (this is the limitation of the FCA, as discussed in the formalism). In fact, we also have two more form factors for the clusters, the f_4 and K_3 states, seen in Table I. Since the form factor often reduces quickly above a certain momentum ($q \simeq 2\Lambda'$), as shown in Fig. 4 (left), we can safely choose the same cutoffs as f_2 and K_1 for those of f_4 and K_3, respectively, to avoid introducing any new free parameters, as seen in Fig. 4 (right). Furthermore, even though we change the value of the determined $q_{\max}$ a bit, for example 10%, if it is still in the nature value [33] (which means that the values of the $q_{\max}$ lead to the dimensional regularization parameter $a(\mu)$ around the value of -2 when taking $\mu = q_{\max}$), the shape of the form factor will not be changed (see Fig. 4). Thus, our final conclusion will not be changed, and only the strength of the amplitude will be a little different.

We have mentioned in the formalism that we should take into account the isospin structure of the subsystems for the two-body amplitudes t_1 and t_2. For the first case of K–$f_2(\rho\rho)$, the cluster of f_2 resonance has isospin $I = 0$. Therefore, the two ρ mesons are in an $I = 0$ state, and we write it in terms of the physical basis components

$$|\rho\rho\rangle^{(0,0)} = \frac{1}{\sqrt{3}}(|(1,-1)\rangle + |(-1,1)\rangle - |(0,0)\rangle), \quad (22)$$

where $|(1,-1)\rangle$ denotes $|(I_z^1, I_z^2)\rangle$, which shows the I_z components of particles 1 and 2, and $|\rho\rho\rangle^{(0,0)}$ means $|\rho\rho\rangle^{(I,I_z)}$. Then, the third particle is a K meson taken $|I_z^3\rangle = |\frac{1}{2}\rangle$, obtained as follows:

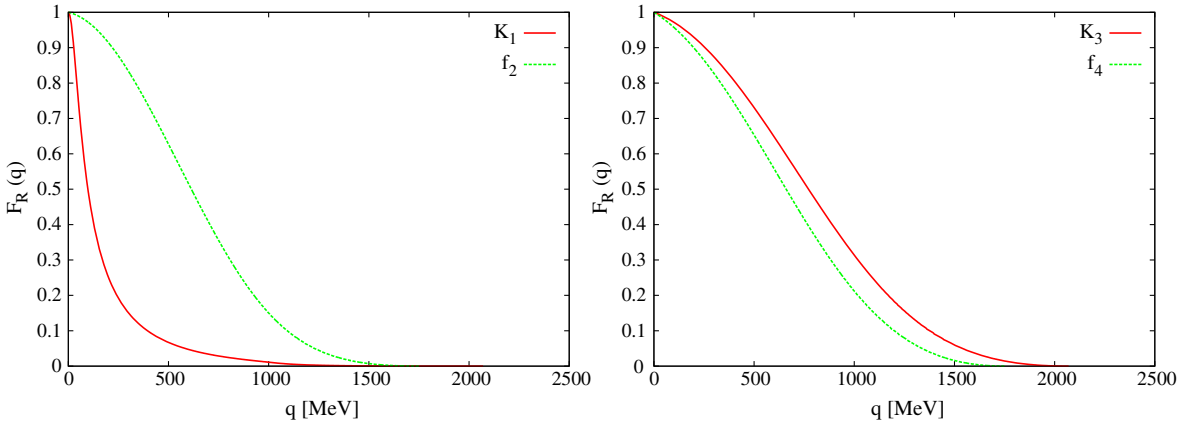

FIG. 4 (color online). The form factors of $f_2(1270)$ and $K_1(1270)$ (left), $f_4(2050)$ and $K_3(2080)$ (right).

$$
\begin{aligned}
T^{(\frac{1}{2},\frac{1}{2})}_{K-f_2} &= \langle K-\rho\rho|\hat{t}|K-\rho\rho\rangle^{(\frac{1}{2},\frac{1}{2})} \\
&= (\langle K|^{(\frac{1}{2},\frac{1}{2})}\otimes\langle\rho\rho|^{(0,0)})(\hat{t}_{31}+\hat{t}_{32})(|K\rangle^{(\frac{1}{2},\frac{1}{2})}\otimes|\rho\rho\rangle^{(0,0)}) \\
&= \left[\left\langle\frac{1}{2}\right|\otimes\frac{1}{\sqrt{3}}(\langle(1,-1)|+\langle(-1,1)|-\langle(0,0)|)\right](\hat{t}_{31}+\hat{t}_{32})\left[\left|\frac{1}{2}\right\rangle\otimes\frac{1}{\sqrt{3}}(|(1,-1)\rangle+|(-1,1)\rangle-|(0,0)\rangle)\right] \\
&= \frac{1}{3}\left[\left\langle\left(\frac{3}{2},\frac{3}{2}\right),-1\right|+\sqrt{\frac{1}{3}}\left\langle\left(\frac{3}{2},-\frac{1}{2}\right),1\right|+\sqrt{\frac{2}{3}}\left\langle\left(\frac{1}{2},-\frac{1}{2}\right),1\right|-\sqrt{\frac{2}{3}}\left\langle\left(\frac{3}{2},\frac{1}{2}\right),0\right|\right. \\
&\quad \left.-\sqrt{\frac{1}{3}}\left\langle\left(\frac{1}{2},\frac{1}{2}\right),0\right|\right]\hat{t}_{31}\left[\left|\left(\frac{3}{2},\frac{3}{2}\right),-1\right\rangle+\sqrt{\frac{1}{3}}\left|\left(\frac{3}{2},-\frac{1}{2}\right),1\right\rangle+\sqrt{\frac{2}{3}}\left|\left(\frac{1}{2},-\frac{1}{2}\right),1\right\rangle\right. \\
&\quad \left.-\sqrt{\frac{2}{3}}\left|\left(\frac{3}{2},\frac{1}{2}\right),0\right\rangle-\sqrt{\frac{1}{3}}\left|\left(\frac{1}{2},\frac{1}{2}\right),0\right\rangle\right]+\frac{1}{3}\left[\sqrt{\frac{1}{3}}\left\langle\left(\frac{3}{2},-\frac{1}{2}\right),1\right|+\sqrt{\frac{2}{3}}\left\langle\left(\frac{1}{2},-\frac{1}{2}\right),1\right|\right. \\
&\quad +\left\langle\left(\frac{3}{2},\frac{3}{2}\right),-1\right|-\sqrt{\frac{2}{3}}\left\langle\left(\frac{3}{2},\frac{1}{2}\right),0\right|-\sqrt{\frac{1}{3}}\left\langle\left(\frac{1}{2},\frac{1}{2}\right),0\right|\left.\right]\hat{t}_{32}\left[\sqrt{\frac{1}{3}}\left|\left(\frac{3}{2},-\frac{1}{2}\right),1\right\rangle\right. \\
&\quad \left.+\sqrt{\frac{2}{3}}\left|\left(\frac{1}{2},-\frac{1}{2}\right),1\right\rangle+\left|\left(\frac{3}{2},\frac{3}{2}\right),-1\right\rangle-\sqrt{\frac{2}{3}}\left|\left(\frac{3}{2},\frac{1}{2}\right),0\right\rangle-\sqrt{\frac{1}{3}}\left|\left(\frac{1}{2},\frac{1}{2}\right),0\right\rangle\right], \qquad (23)
\end{aligned}
$$

where the notation of the states followed in the terms is $|(\frac{3}{2},\frac{3}{2}),-1\rangle \equiv |(I^{31},I_z^{31}),I_z^2\rangle$ for t_{31}, and $|(I^{32},I_z^{32}),I_z^1\rangle$ for t_{32}. Finally, we obtain the amplitudes combining with the isospin structure

$$
t_1 = t_{\rho K} = \frac{1}{3}(2t_{31}^{I=3/2}+t_{31}^{I=1/2}), \qquad t_2 = t_1, \qquad (24)
$$

where ρK scattering amplitudes with isospin $I=1/2,3/2$, $t_{31}^{I=1/2}$, and $t_{31}^{I=3/2}$ have been evaluated in Sec. III B.

But for the second case of ρ–$K_1(\rho K)$, the isospin structure relationship is different. Now, the isospins of ρ and K_1 are $I_\rho = 1$ and $I_{K_1} = \frac{1}{2}$; thus, the total isospin of the three-body system is expressed by the two cases $I_{\text{total}} \equiv I_{\rho\rho K} = \frac{1}{2}$ and $I_{\text{total}} \equiv I_{\rho\rho K} = \frac{3}{2}$. Therefore, we have

$$
\begin{aligned}
|\rho K_1\rangle^{(\frac{1}{2},\frac{1}{2})} &= |\rho\rho K\rangle^{(\frac{1}{2},\frac{1}{2})} = \sqrt{\frac{2}{3}}\left|\left(1,-\frac{1}{2}\right)\right\rangle-\sqrt{\frac{1}{3}}\left|\left(0,\frac{1}{2}\right)\right\rangle, \\
|\rho K_1\rangle^{(\frac{3}{2},\frac{1}{2})} &= |\rho\rho K\rangle^{(\frac{3}{2},\frac{1}{2})} = \sqrt{\frac{1}{3}}\left|\left(1,-\frac{1}{2}\right)\right\rangle+\sqrt{\frac{2}{3}}\left|\left(0,\frac{1}{2}\right)\right\rangle,
\end{aligned} \qquad (25)
$$

where we have taken the third isospin component $I_z = \frac{1}{2}$ for convenience. Then the $|\rho K\rangle$ states inside the K_1 for the $I_z = -\frac{1}{2}$ and $I_z = +\frac{1}{2}$ are given by

$$
\begin{aligned}
|\rho K\rangle^{(\frac{1}{2},-\frac{1}{2})} &= \sqrt{\frac{1}{3}}\left|\left(0,-\frac{1}{2}\right)\right\rangle-\sqrt{\frac{2}{3}}\left|\left(-1,\frac{1}{2}\right)\right\rangle, \\
|\rho K\rangle^{(\frac{1}{2},\frac{1}{2})} &= \sqrt{\frac{2}{3}}\left|\left(1,-\frac{1}{2}\right)\right\rangle-\sqrt{\frac{1}{3}}\left|\left(0,\frac{1}{2}\right)\right\rangle.
\end{aligned} \qquad (26)
$$

For the two possibilities, using Eqs. (25) and (26) and performing a similar derivation of Eq. (27), we obtain

$$
\begin{aligned}
T^{(I=1/2)}_{\rho-K_1}:\ t_1 &= t_{\rho\rho} = \frac{2}{3}t_{31}^{I=0}, \\
t_2 &= t_{\rho K} = \frac{1}{9}(8t_{32}^{I=3/2}+t_{32}^{I=1/2}); \\
T^{(I=3/2)}_{\rho-K_1}:\ t_1 &= t_{\rho\rho} = \frac{5}{6}t_{31}^{I=2}, \\
t_2 &= t_{\rho K} = \frac{1}{9}(5t_{32}^{I=3/2}+4t_{32}^{I=1/2}),
\end{aligned} \qquad (27)
$$

where $\rho\rho$ interaction amplitudes with isospin $I=0,2$, $t_{31}^{I=0}$, and $t_{31}^{I=2}$ are evaluated in Sec. III A, and those of ρK interaction, $t_{32}^{I=1/2}$ and $t_{32}^{I=3/2}$, are given in Sec. III B.

In Fig. 5, we show our results of the modulus squared of the amplitude for $|T^{I=1/2}_{K-f_2}|^2$. There is a clear and sharp peak

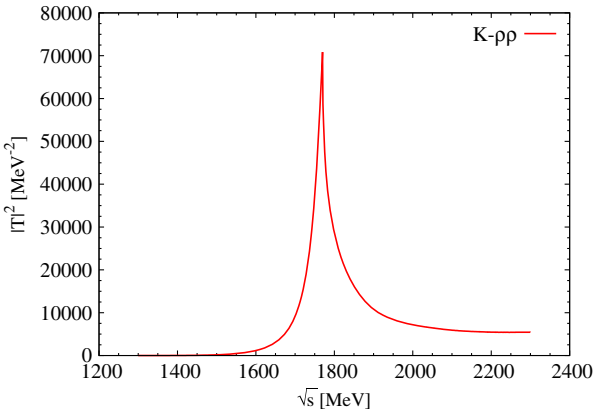

FIG. 5 (color online). Modulus squared of the T_{K-f2}.

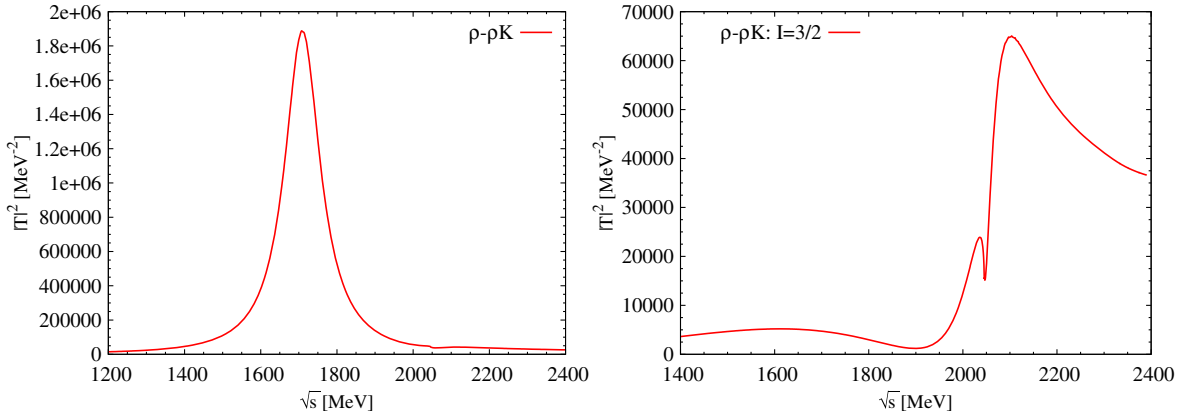

FIG. 6 (color online). Modulus squared of the $T_{\rho-K_1}$ scattering amplitudes. Left: $I_{\rm total}=\frac{1}{2}$. Right: $I_{\rm total}=\frac{3}{2}$.

around 1770 MeV, which is close to the threshold of K–f_2 and similar to a cusp in the case of the $\eta' K\bar{K}$ system [81]. Therefore, this peak in $|T^{I=1/2}_{K-f_2}|^2$ would be affected by the threshold effect, and the width of this resonance structure has large uncertainties. There would be the cusp corresponding to a real resonance in some cases, like $a_0(980)$ [28] (more discussions about the states appearing near the threshold can be found in the recent works of Refs. [82,83]). In Fig. 6, we show the results of $|T^{I=1/2}_{\rho-K_1}|^2$ (left) and $|T^{I=3/2}_{\rho-K_1}|^2$ (right). From the $|T^{I=1/2}_{\rho-K_1}|^2$ results, we find that there is a clear peak around the energy 1707 MeV with a width about 113 MeV,[2] which is about 340 MeV below the ρ–K_1 threshold and the $\rho\rho K$ threshold. Because of the large width of the ρ meson, for a system with two ρ mesons, the large bindings in the present case will be acceptable. In the PDG data [60], the $K_2(1770)$ of $J^P=2^-$ strangeness state is the mass of 1773 ± 8 MeV and the width 186 ± 14 MeV. But from the analysis of the $K\omega$ spectrum in the reaction $K^- p\to K^-\omega p$, the work of Ref. [85] obtains its mass as 1710 ± 15 MeV and width 110 ± 50 MeV, which is consistent with our results. Our results are also consistent with the other experimental results [86–88]. Thus, considering the uncertainties in our study (which will be discussed later), the peak appearing in the $|T^{I=1/2}_{\rho-K_1}|^2$ case corresponds to $K_2(1770)$, which would be the ρ–K_1 molecular state in our model. The strength of the peak of $|T^{I=1/2}_{K-f_2}|^2$ is about 25 times smaller than for $|T^{I=1/2}_{\rho-K_1}|^2$; thus, we could not expect a state structure in Fig. 5, even though the two-body interaction of ρK is not as strong as $\rho\rho$, as can be seen by comparing the results of Figs. 2 and 3. From the results of $|T^{I=3/2}_{\rho-K_1}|^2$ in Fig. 6 (right), we can see that there is a clear resonant structure about 2100 MeV with the strength 25 times smaller than that of $|T^{I=1/2}_{\rho-K_1}|^2$ in the left figure, which is a little above the ρ–$K1(1270)$ threshold, and also shows a dip in the threshold. We are looking for the lowest-lying states bound in the K–multi-ρ system, and hence, we could not expect a new state in the $|T^{I=3/2}_{\rho-K_1}|^2$ results.

B. Four-body interaction

For the four-body interaction as shown in Table I, we also have two possibilities: (i) particle $3=f_2$, cluster $R=K_1$ $(1=\rho, 2=K)$; or (ii) particle $3=K_1$, resonance $R=f_2$ $(1=\rho, 2=\rho)$. Because the isospins of the two clusters are $I_{f_2}=0$ and $I_{K_1}=\frac{1}{2}$, the total isospin of the four-body system is only $I_{\rm total}=\frac{1}{2}$. Using the FCA formalism as discussed in Sec. II for the four-body interaction, for the first option, f_2 interacting with the K_1, we need to evaluate the amplitudes $t_1=t_{f_2\rho}=T_{\rho-f_2}$, which has been done in Ref. [41],[3] and $t_2=t_{f_2K}=T_{K-f_2}$, which has been calculated above in Sec. IV A. Similarly, for the second case, K_1 collides with the f_2, and the amplitudes $t_1=t_2=t_{K_1\rho}=T_{\rho-K_1}$ have been evaluated in Sec. IV A. Note that the three-body amplitude $T_{\rho-K_1}$ should be also written in terms of the isospin structure as discussed in Sec. II and its amplitudes of isospin components evaluated in Sec. IV A. Since the isospins of both K_1 and K are $I=\frac{1}{2}$, the isospin structure is similar to the case when the K collides with the f_2. Thus, analogously to Eq. (24), we have

$$t_1=T_{\rho K_1}=\frac{1}{3}(2T^{I=3/2}_{31}+T^{I=1/2}_{31}),\qquad t_2=t_1. \tag{28}$$

We show our results in Fig. 7, of which the left panel is $|T^{I=1/2}_{f_2-K_1}|^2$ and the right panel $|T^{I=1/2}_{K_1-f_2}|^2$, where the clusters

[2]Because of the complicated situation in the definition of the second Riemann sheets in the multibody interaction, we have difficulty extracting the masses by the poles in the second Riemann sheets, which is different from the two-body interaction; more discussion can be seen in Ref. [84]. Thus, we extract the mass and the width from the scattering amplitude in the first Riemann sheet, shown in the figures.

[3]Where they used a similar formalism of Sec. II. Thus, using the formalism of Sec. II and the $\rho\rho$ interaction amplitudes in Sec. III A, we can reproduce their results.

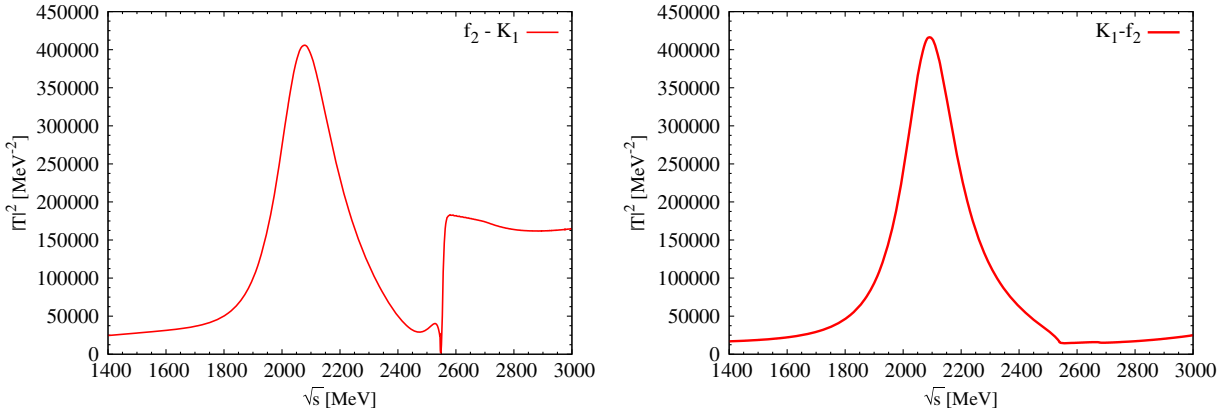

FIG. 7 (color online). Modulus squared of the $T_{f_2-K_1}$ (left) and T_{K_1-f2} (right) scattering amplitudes.

are the resonances K_1 and f_2, respectively. In the left panel of Fig. 7, there is a clear peak at an energy of about 2079 MeV, the width of which is about 249 MeV. We also find discontinuity at the position about 2550 MeV, which comes from the contribution of the f_2–K_1 threshold effect. In the right panel of Fig. 7, we also find that there is a resonant peak around the energy 2091 MeV with a width of 230 MeV in the $|T^{I=1/2}_{K_1-f_2}|^2$. The strength of the peak of $|T^{I=1/2}_{K_1-f_2}|^2$ is at the same magnitude as that of $|T^{I=1/2}_{f_2-K_1}|^2$, and the energy of the peak is a little less bound. In the PDG data, there is only one $J^P = 3^+ K_3$ state found in the experiments, $K_3(2320)$, with a mass 2324 ± 24 MeV and width 150 ± 30 MeV. This $K_3(2320)$ state was just found in the reactions $K^+p \to (\bar{\Lambda}p)p$ and $K^-p \to (\Lambda\bar{p})p$ [89,90]. But its mass is too far away from our results. Therefore, we find a new K_3 state with uncertainties, with a mass about 2079–2091 MeV and a width about 230–249 MeV.

C. Five-body interaction

As we expected before, we also find a new K_3 state in the four-body interaction in Sec. IV B. Thus, for the five-body interaction, there also are two options for the cluster, one of which is the f_4 state found in the PDG data and studied in Ref. [41]; and the other, which is the resonance K_3 obtained in the four-body interaction above. Then following the idea of FCA and letting the third particle (K or ρ) collide with them, the two possibilities are (i) particle $3 = K$, cluster $R = f_4$ $(1 = f_2, 2 = f_2)$; or (ii) $3 = \rho$, $R = K_3$ $(1 = f_2, 2 = K_1)$. Since the isospin $I_{f_4} = 0$ and $I_{K_3} = \frac{1}{2}$, for the first case, the total isospin of the K–f_4 system is only $I_{\text{total}} = \frac{1}{2}$; but for the second option ρ–K_3, the total isospin of this structure is $I_{\text{total}} = \frac{1}{2}$ or $I_{\text{total}} = \frac{3}{2}$. Therefore, the situation of K interacting with f_4 (K–f_4) is similar to the three-body interaction discussed before, K colliding with f_2 (K–f_2), and ρ–K_3 is analogous to the case of ρ–K_1. Thus, in the first case, the K collides with the f_4, and the amplitudes $t_1 = t_2 = t_{Kf_2} = T^{(I=1/2)}_{K-f_2}$ have been evaluated in Sec. IV A for the three-body interaction. For the second case, the ρ interacts with the K_3, which is similar to ρ–K_1 in Sec. IV A. Thus, doing a similar derivation as done in Eq. (23), we obtain

$$\begin{aligned} T^{(I=1/2)}_{\rho-K_3}&: t_1 = t_{\rho f_2} = T^{(I=1)}_{31}, \qquad t_2 = t_{\rho K_1} = T^{I=1/2}_{32}; \\ T^{(I=3/2)}_{\rho-K_3}&: t_1 = t_{\rho f_2} = T^{(I=1)}_{31}, \qquad t_2 = t_{\rho K_1} = T^{I=3/2}_{32}, \end{aligned} \tag{29}$$

where $T^{(I=1)}_{31}$ is the amplitude of $T_{\rho-f_2}$, which is the same as that calculated in Sec. IV B, reproducing the results of Ref. [41], and the amplitudes $T^{I=1/2}_{\rho-K_1}$ and $T^{I=3/2}_{\rho-K_1}$ have also been evaluated in Sec. IV A.

We show our results for the two cases of the five-body interaction in Fig. 8. The results of $|T^{I=1/2}_{K-f_4}|^2$ are shown on the left of Fig. 8, where we can see a resonant peak around the energy 2505 MeV with a width of about 32 MeV. The right of Fig. 8 shows the results of $|T^{I=1/2}_{\rho-K_3}|^2$ and $|T^{I=3/2}_{\rho-K_3}|^2$. We observe that there are clear peaks for both of them. A resonant structure in $|T^{I=1/2}_{\rho-K_3}|^2$ is found at the energy 2382 MeV with the width about 409 MeV, which is about 120 MeV more bound than that of $|T^{I=1/2}_{K-f_4}|^2$ and a much larger width too. But the strength of $|T^{I=1/2}_{\rho-K_3}|^2$ is just $\frac{1}{2}$ smaller than that of $|T^{I=1/2}_{K-f_4}|^2$. Thus, the more bound energy and larger width in $|T^{I=1/2}_{\rho-K_3}|^2$ come from the stronger $\rho\rho$ interaction in the components of the K_3 state, which we can see from Figs. 2 and 3. In experiments, one $J^P = 4^-$ state was also found in Ref. [89], $K_4(2500)$, with the mass 2490 ± 20 MeV and width around 250 MeV, which is not well confirmed in the PDG data because of the lack of more experimental information. This $K_4(2500)$ state is dynamically generated as a molecular state of K–f_4 in our results of $|T^{I=1/2}_{K-f_4}|^2$, with a mass 2505 MeV and a width about 32 MeV. The predicted width of our results is 8 times smaller than the one reported. We should admit that there

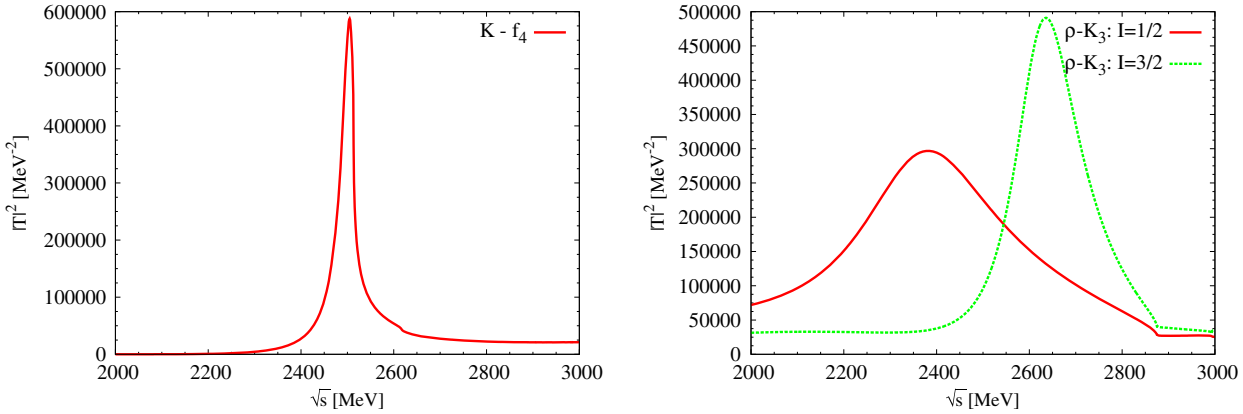

FIG. 8 (color online). Modulus squared of the T_{K-f_4} (left) and $T_{\rho-K_3}$ (right) scattering amplitudes.

are also uncertainties in our results, seen from the results of $|T^{I=1/2}_{\rho-K_3}|^2$ in the right panel of Fig. 8 and discussed later. For $|T^{I=3/2}_{\rho-K_3}|^2$, there is also resonant structure at the position about 2636 MeV, the width of which is about 171 MeV, which is not found for any $I = 3/2$ K_4 state in the PDG data. Thus, within uncertainties, we predict a new K_4 resonance of isospin $I = 3/2$, with a mass about 2636 MeV and a width about 171 MeV.

D. Six-body interaction

From Table I, if we predict a K_3 state, seen in Sec. IV B, analogously to the five-body interaction, there are also two options of the cluster for the six-body interaction: the particle f_4 found in the PDG data and studied in Ref. [41], and the resonance K_3 predicted above. Under the FCA, we let a third particle of the composite resonance (K_1 or f_2) collide with them, creating (i) particle $3 = K_1$, cluster $R = f_4$ $(1 = f_2, 2 = f_2)$; or (ii) $3 = f_2$, $R = K_3$ $(1 = f_2, 2 = K_1)$. Since the isospin of the particles $I_{f_2} = I_{f_4} = 0$ and $I_{K_1} = I_{K_3} = \frac{1}{2}$, we find that the total isospin of the six-body system is only $I_{\text{total}} = \frac{1}{2}$. Thus, for the first case, the K_1 colliding with the f_4 (K–f_4), we need to calculate the amplitudes $t_1 = t_2 = t_{K_1 f_2} = T^{(I=1/2)}_{K_1-f_2}$, which have been evaluated in Sec. IV B. For the second case, the f_2 colliding with the K_3, we evaluate the amplitudes $t_1 = t_{f_2 f_2} = T_{f_2-f_2}$ by reproducing the results of Ref. [41] within our formalism (we have already reproduced $T_{\rho-f_2}$ in Sec. IV B), and $t_2 = t_{f_2 K_1} = T_{f_2-K_1}$, from the results of Sec. IV B.

We show our results for the six-body interaction in Fig. 9. The left panel of Fig. 9 is $|T^{I=1/2}_{K_1-f_4}|^2$. Since K_1 collides with the f_4, with the amplitudes $t_1 = t_2 = t_{K_1 f_2} = T^{(I=1/2)}_{K_1-f_2}$, as shown in Sec. IV B, the amplitude $T^{(I=1/2)}_{K_1-f_2} \neq T^{(I=1/2)}_{f_2-K_1}$; for a test we also take $t_1 = t_2 = t_{K_1 f_2} = T^{(I=1/2)}_{f_2-K_1}$ to evaluate the scattering amplitude again. By taking $t_1 = t_2 = t_{K_1 f_2} = T^{(I=1/2)}_{K_1-f_2}$, we find a peak around the energy 2558 MeV with a large width of about 531 MeV. For the results of taking $t_1 = t_2 = t_{K_1 f_2} = T^{(I=1/2)}_{f_2-K_1}$, there also is a resonant peak in the position about 2670 MeV, the width of which is about 543 MeV. We can see that this test just gives us some uncertainties for our results. The right panel of Fig. 9 is $|T^{I=1/2}_{f_2-K_3}|^2$, where we can

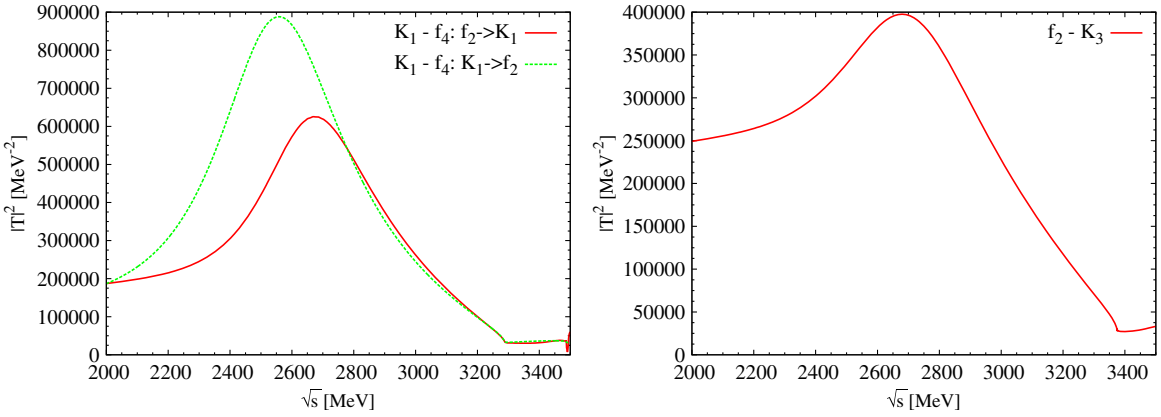

FIG. 9 (color online). Modulus squared of the $T_{K_1-f_4}$ (left) and $T_{f_2-K_3}$ (right) scattering amplitudes.

observe that there is not a clear peak at the position 2681 MeV. This peak looks like the resonant structure of f_2–K_3, which is less stable compared with that of K_1–f_4. Since there was no K_5 particle found by PDG, there could be a new K_5 resonance which causes more uncertainty from our results, with a mass of about 2558–2681 MeV and a large width about 531–543 MeV or more.

E. Discussions

Now, we would like to have a discussion about the uncertainties of our results. As discussed in Sec. III, we have considered the width of the vector mesons in the evaluation of the two-body interaction amplitudes, $t_{\rho\rho}$ and $t_{\rho K}$, by taking into account the convolution of the loop function G^I. On the other hand, for the K–multi-ρ system in the present work, the third particle in many cases, seen in Table I, is a vector meson or a resonance, and has a large width, which should be taken into account. Thus, as is done in Ref. [48], we can roughly consider the width of the third particle in the propagator function G_0 [Eq. (5)] by replacing the term in the denominator $i\epsilon$ with $im_3\Gamma_3$. Or, we can do the convolution of the G_0 function for considering more exactly the contribution of the width of the third particle, as is done in Ref. [84]. But, as shown in the results of Refs. [48,84], the final results for the position of the generated states are not altered after considering the contribution of the width of the third particle, to which we assign some uncertainties on the width for the generated results. Furthermore, there is also certain width for the clusters—for example, the resonances of $f_2(1270)$ and $K_1(1270)$ in the three-body interaction—which have a big width. As is done in Refs. [48,84], we also would take into account roughly the contribution of the width of the cluster by replacing the mass of the cluster M_R in Eqs. (7) and (8) with $M_R - i\Gamma_R/2$. In fact, the contribution for the width of the cluster is just a small effect on the masses and widths of the generated results (see Refs. [48,84] for more discussion). For checking this contribution, we also can consider the convolution for the t_i, since Eq. (16) is dependent on the mass of the cluster, as seen in Fig. 10 taking K–$\rho\rho$ scattering for example, where we can see that the effect of the width of the cluster is small for the position of the peak and just makes the width of the peak a bit larger. Therefore, in our present work, we ignore all these effects in our investigation, just keeping in mind that there are also some uncertainties from considering the contribution of the width of the third particle and the cluster. Besides, according to the discussions in Ref. [91], there may be some uncertain effect in the denominator term of $\tilde{t}_1\,\tilde{t}_2\,G_0^2$ ($\tilde{t}_1 G_0$) in Eq. (14) [Eq. (15)].

We would like to have some discussion concerning the off-shell contributions in our formalism. For the two-body interactions, we follow the works of Refs. [65,67] for the $\rho\rho$ and ρK interactions, where the on-shell Bethe-Salpeter equation was used. A short proof of the on-shell

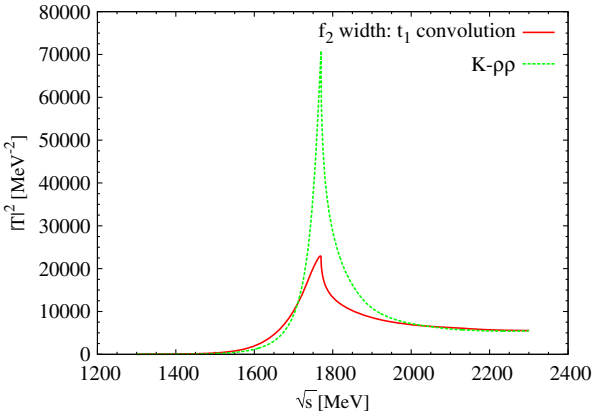

FIG. 10 (color online). Considering the convolution of t_i in the K–$\rho\rho$ scattering amplitudes.

Bethe-Salpeter equation is given in Refs. [28,29], and a different justification is given in Ref. [33], where a subtracted dispersion relation is used and one can obtain the results of the on-shell Bethe-Salpeter equation when one neglects the contribution of the left-hand cut. Besides, the on-shell approximation and full off-shell effects are discussed in detail in Ref. [92] for $\pi\pi$ scattering and in the works of the Bonn group [93–95]. In the present work, we investigate the K–multi-ρ interactions with the FCA to Faddeev equations, which are different from the full Faddeev equations with ChUA, as used in Ref. [39]. One of the intrinsic differences between them is that the FCA to Faddeev equations are based on the two-body on-shell amplitudes as input, while the full Faddeev equations use the full off-shell amplitudes. Yet this should not be seen as a drawback of the FCA. Indeed, in the full Faddeev equation calculations of Ref. [39], the full off-shell amplitudes can be separated into two parts: an on-shell part, and a remnant off-shell part, which are unphysical. In full Faddeev calculations these unphysical parts will be implicitly canceled by *ad hoc* three-body forces which are included in the calculations, details seen in Refs. [96,97]. This means that using the on-shell amplitudes in the Faddeev equations is a more appropriate way to deal with the three-body system than using the full-off shell amplitudes if no additional three-body forces are introduced [52]. The use of the on-shell amplitudes in the FCA gets a strong support from these findings. Indeed, since the on-shell two-body amplitudes are used as input in the FCA to Faddeev equations, the cancellation of the off-shell contribution cannot hold as in the full Faddeev equation calculations [39]. Up to one loop, there are only two diagrams, seen in Figs. 1(b) and 1(f), while the full Faddeev equation calculations have six diagrams. Following Ref. [39], we divide the on-shell and off-shell parts for the two-body amplitudes, written $t_i(s_i) = t_i^{\rm on}(s_i) + t_i^{\rm off}(s_i)$; thus, using Eq. (11) we have for one loop

$$T_1^{(b)}(T_2^{(f)}) \sim \int \frac{d^3q}{(2\pi)^3} F_R(\vec{q}) \frac{1}{q^{02} - \vec{q}^2 - m_3^2 + i\epsilon} \times (t_1^{\rm on} + t_1^{\rm off})(t_2^{\rm on} + t_2^{\rm off}), \quad (30)$$

where we can see that the off-shell parts of the two-body amplitudes cannot be canceled, since we do not have the interaction force from the contact terms. But one can also see that, because of the constraints of the form factor $F_R(\vec{q})$ (seen in Fig. 4), the contribution of the off-shell parts cannot be infinity. The results of Ref. [98] (in their Fig. 6) show that the position of the peak $m_{\rm peak}$ move to higher less than 3% when one takes a q_i dependent to $t_i(s_i)$. Thus, the contribution of the off-shell parts are small, which can be included in our uncertainties.

V. CONCLUSIONS

In the present work, we investigate the many-body interactions in K–multi-ρ systems, using the formalism of the fixed-center approximation to the Faddeev equations. We start from the two-body interaction of $\rho\rho$ and ρK with the combination of dynamics of the local hidden gauge Lagrangian and the coupled channel effect, to reproduce the resonances of $f_2(1270)$ and $K_1(1270)$ as the clusters for our formalism. We summarize our results in Table II, where we obtain some bound states in the K–multi-ρ interactions, as the findings of the three-body wave functions in a finite volume in Ref. [99]. In the three-body $K\rho\rho$ system, we dynamically generate the $K_2(1770)$ state in our formalism, obtain a resonant peak in the modulus squared of the scattering amplitudes around the position in 1707 MeV with a width about 113 MeV, and explain its structure as a ρ–$K_1(1270)$ molecular state. Continuing with the three-body Faddeev equations with the fixed-center approximation, we extrapolate our formalism to the four-body interaction. We observe a new K_3 state, with a mass about 2079–2091 MeV and a width about 230–249 MeV, which would be a K_1–f_2 molecular resonance and is not found in the PDG yet. For the five-body interaction, we successfully generate the $K_4(2500)$ state in our results of $|T^{I=1/2}_{K-f_4}|^2$, with a mass 2505 MeV and a width about 32 MeV, even though our theoretically predicted width is smaller than that of unconfirmed experimental results of about 250 MeV. Thus, we also explain the structure of $K_4(2500)$ as a molecular state of K–f_4. Besides, we find a new K_4 resonance of isospin $I = 3/2$ in the ρ–K_3 interaction, with a mass about 2636 MeV and a width about 171 MeV. Finally, analogously, we predict a new K_5 state in the six-body interactions of K_1–f_4 and f_2–K_3, with a mass of about 2558–2681 MeV and a large width about 531–543 MeV or more, with more uncertainties. We hope that in future experiments, our predicted states of $K_3(2080)$, $K_5(2670)$ (isospin $I = 1/2$), and $K_4(2640)$ (isospin $I = 3/2$) are found.

TABLE II. Our results of the K–multi-ρ interactions (units: MeV).

	Interactions	Results (mass, width)	PDG	Predictions
Three-body	K–$f_2(\rho\rho)$	Cusp	⋯	⋯
	ρ–$K_1(\rho K)^{I=1/2}$	(1707, 113)	$K_2(1770)$	⋯
	ρ–$K_1(\rho K)^{I=3/2}$	⋯	⋯	⋯
Four-body	f_2–$K_1(\rho K)$	(2079, 249)	⋯	
	K_1–$f_2(\rho\rho)$	(2091, 230)	⋯	$K_3(2080)$
Five-body	K–$f_4(f_2f_2)$	(2505, 32)	$K_4(2500)$	⋯
	ρ–$K_3(f_2K_1)^{I=1/2}$	(2382, 409)		⋯
	ρ–$K_3(f_2K_1)^{I=3/2}$	(2636, 171)	⋯	$K_4(2640)$
Six-body	K_1–$f_4(f_2f_2)$	(2558–2670, 531–543)	⋯	$K_5(2670)$
	f_2–$K_3(f_2K_1)$	(2681, > 500)	⋯	

ACKNOWLEDGMENTS

We thank M. J. Vicente Vacas for useful discussions, and also appreciate E. Oset, C. Hanhart, and Ulf-G. Meißner for careful reading of the paper and useful comments. This work is supported, in part, by NSFC and DFG through funds provided to the Sino-German CRC 110 "Symmetries and the Emergence of Structure in QCD." This work is also partly supported by the Spanish Ministerio de Economia y Competitividad and European FEDER funds under Contract No. FIS2011-28853-C02-01 and the Generalitat Valenciana in the program Prometeo No. 2009/090. We acknowledge the support of the European Community-Research Infrastructure Integrating Activity Study of Strongly Interacting Matter (Hadron Physics 3, Grant No. 283286) under the Seventh Framework Programme of the European Union.

APPENDIX A: CONTRIBUTION OF THE BOX DIAGRAM AND THE CONVOLUTION OF THE LOOP

As mentioned in Ref. [65], we should take into account the contribution of the box diagram to the potential V^I. The main contribution is the $\pi\pi$ box diagram for $\rho\rho$ interaction, written

$$V^{(2\pi,I=0,S=2)}_{\rm box(\rho\rho)}(s) = 8\tilde{V}^{(\pi\pi)}, \quad (A1)$$

where $\tilde{V}^{(\pi\pi)}$ is given by

$$\tilde{V}^{(\pi\pi)}(s) = (\sqrt{2}g)^4 \frac{8}{15\pi^2} \int_0^{q'_{\rm max}} dq\vec{q}^6 [10\omega^2 - (k_3^0)^2] \frac{1}{\omega^3} \times \left(\frac{1}{k_1^0 + 2\omega}\right)^2 \frac{1}{P^0 + 2\omega} \frac{1}{k_1^0 + \frac{\Gamma}{4} - 2\omega + i\epsilon} \times \frac{1}{k_1^0 - \frac{\Gamma}{4} - 2\omega + i\epsilon} \frac{1}{P^0 - 2\omega + i\epsilon} F(q)^4, \quad (A2)$$

where $\omega = \sqrt{\vec{q}^2 + m_\pi^2}$ and $\sqrt{s} = P^0 = k_1^0 + k_2^0$. For the cutoff in the integration, we took a natural size, $q'_{\max} = 1200$ MeV. Besides this, $F(q)$ is a form factor for an off-shell π in each vertex, in the case of the $\pi\pi$ box, taken as

$$F(q) = \frac{\Lambda^2 - m_\pi^2}{\Lambda^2 + \vec{q}^2}, \tag{A3}$$

with $\Lambda = 1300$ MeV.

The element of the loop function in the matrix G^I in Eq. (19) is only a two-meson loop, read

$$G^I_{ii}(s, m_1, m_2) = i \int \frac{d^4q}{(2\pi)^4} \frac{1}{q^2 - m_1^2 + i\epsilon} \frac{1}{(P-q)^2 - m_2^2 + i\epsilon}, \tag{A4}$$

which could be regularized by the cutoff, obtained from

$$G^I_{ii}(s, m_1, m_2) = \int_0^{q_{\max}} \frac{\vec{q}^2 d|\vec{q}|}{(2\pi)^2} \frac{\omega_1 + \omega_2}{\omega_1 \omega_2 [(P^0)^2 - (\omega_1 + \omega_2)^2 + i\epsilon]}, \tag{A5}$$

where $\omega_i = \sqrt{\vec{q}^2 + m_i^2}$, the center-of-mass energy $(P^0)^2 = s$, and $q_{\max}$ stands for the cutoff, for which we took $q_{\max} = 875$ MeV for the $\rho\rho$ interaction. Notice that we also could do the calculation of Eq. (A5) with the analytic expressions in Refs. [31,80]. But we need to take into account the convolution due to the ρ mass distribution by replacing the G function as follows:

$$\begin{aligned}\tilde{G}_{\rho\rho}(s) &= \frac{1}{N^2} \int_{(m_\rho - 2\Gamma_\rho)^2}^{(m_\rho + 2\Gamma_\rho)^2} d\tilde{m}_1^2 \left(-\frac{1}{\pi}\right) \\ &\times \mathrm{Im} \frac{1}{\tilde{m}_1^2 - m_\rho^2 + i\tilde{m}_1 \Gamma(\tilde{m}_1)} \int_{(m_\rho - 2\Gamma_\rho)^2}^{(m_\rho + 2\Gamma_\rho)^2} d\tilde{m}_2^2 \left(-\frac{1}{\pi}\right) \\ &\times \mathrm{Im} \frac{1}{\tilde{m}_2^2 - m_\rho^2 + i\tilde{m}_2 \Gamma(\tilde{m}_2)} G_{\rho\rho}(s, \tilde{m}_1^2, \tilde{m}_2^2)\end{aligned} \tag{A6}$$

is replaced with

$$N = \int_{(m_\rho - 2\Gamma_\rho)^2}^{(m_\rho + 2\Gamma_\rho)^2} d\tilde{m}_1^2 \left(-\frac{1}{\pi}\right) \mathrm{Im} \frac{1}{\tilde{m}_1^2 - m_\rho^2 + i\tilde{m}_1 \Gamma(\tilde{m}_1)}, \tag{A7}$$

$$\Gamma(\tilde{m}_1) = \Gamma_\rho \left(\frac{\tilde{m}_1^2 - 4m_\pi^2}{m_\rho^2 - 4m_\pi^2}\right)^{3/2}, \tag{A8}$$

where $\Gamma_\rho = 146.2$ MeV, and $G_{\rho\rho}(s, \tilde{m}_1^2, \tilde{m}_2^2)$ is given by Eq. (A5).

TABLE III. Coefficients C_{ij} in Eq. (20) in the $I = 1/2$ sector.

	ϕK	ωK	ρK	$K^*\eta$	$K^*\pi$
ϕK	0	0	0	$-\sqrt{\frac{3}{2}}$	$-\sqrt{\frac{3}{2}}$
ωK	0	0	0	$\frac{\sqrt{3}}{2}$	$\frac{\sqrt{3}}{2}$
ρK	0	0	−2	$-\frac{3}{2}$	$\frac{1}{2}$
$K^*\eta$	$-\sqrt{\frac{3}{2}}$	$\frac{\sqrt{3}}{2}$	$-\frac{3}{2}$	0	0
$K^*\pi$	$-\sqrt{\frac{3}{2}}$	$\frac{\sqrt{3}}{2}$	$\frac{1}{2}$	0	−2

TABLE IV. Coefficients C_{ij} in Eq. (20) in the $I = 3/2$ sector.

	ρK	$K^*\pi$
ρK	1	1
$K^*\pi$	1	1

APPENDIX B: COEFFICIENTS OF THE POTENTIAL

The coefficients C_{ij} in Eq. (20) for the $I = 1/2$ sector are given and tabulated in Table III. In the $I = 3/2$ sector, the relevant channels are ρK and $K^*\pi$, and the coefficients are given in Table IV.

APPENDIX C: CONVOLUTION OF THE G^I LOOP FUNCTION

Taking the on-shell factorization, the loop function for two mesons is expressed as a function of the energy s, seen in Eq. (A4). To remove the ultraviolet divergence of the loop function, we follow the dimensional regularization scheme

$$\begin{aligned}G_{ll}(s, M_l, m_l) = \frac{1}{16\pi^2} \Bigg\{ &a(\mu) + \ln \frac{M_l^2}{\mu^2} + \frac{m_l^2 - M_l^2 + s}{2s} \ln \frac{m_l^2}{M_l^2} \\ &+ \frac{q_l}{\sqrt{s}} [\ln(s - (M_l^2 - m_l^2) + 2q_l\sqrt{s}) \\ &+ \ln(s + (M_l^2 - m_l^2) + 2q_l\sqrt{s}) \\ &- \ln(-s + (M_l^2 - m_l^2) + 2q_l\sqrt{s}) \\ &- \ln(-s - (M_l^2 - m_l^2) + 2q_l\sqrt{s})] \Bigg\},\end{aligned} \tag{C1}$$

with a momentum q_l determined at the center-of-mass frame

$$q_l = \frac{\sqrt{[s - (M_l - m_l)^2][s - (M_l + m_l)^2)]}}{2\sqrt{s}}, \tag{C2}$$

where μ is a scale parameter in this scheme. The finite part of the loop function is stable against changes of μ due to the subtraction constant $a(\mu)$, which absorbs the changes of μ, where we take the following parameter set chosen to reproduce $K_1(1270)$ in Ref. [67]:

$$\mu = 900\,\mathrm{MeV}, \quad a(\mu) = -1.85, \quad f = 115\,\mathrm{MeV}. \tag{C3}$$

But, considering a finite width of the vector mesons in the loop function, as is done in Ref. [67], the effect of the propagation of unstable particles is taken into account in terms of the Lehmann representation, which is done by the dispersion relation with its imaginary part

$$D(s) = \int_{s_{\mathrm{th}}}^{\infty} ds_V \left(-\frac{1}{\pi}\right) \frac{\mathrm{Im}D(s_V)}{s - s_V + i\epsilon}, \tag{C4}$$

where s_{th} stands for the square of the threshold energy. Now the spectral function is taken as

$$\mathrm{Im}D(s_V) = \mathrm{Im}\left\{\frac{1}{s_V - M_V^2 + iM_V\Gamma_V}\right\}, \tag{C5}$$

where the width Γ_V is assumed to be a constant physical value. Substituting Eqs. (C4) and (C5) into the original loop function, Eq. (C1), we have

$$\tilde{G}_{ll}(s, M_l, m_l) = \frac{1}{C_l} \int_{(M_l - 2\Gamma_l)^2}^{(M_l + 2\Gamma_l)^2} ds_V G_{ll}(s, \sqrt{s_V}, m_l) \times \left(-\frac{1}{\pi}\right) \mathrm{Im}\left\{\frac{1}{s_V - M_l^2 + iM_l\Gamma_l}\right\}, \tag{C6}$$

where G_{ll} is given by Eq. (C1), and the normalization for the lth component is

$$C_l = \int_{(M_l - 2\Gamma_l)^2}^{(M_l + 2\Gamma_l)^2} ds_V \times \left(-\frac{1}{\pi}\right) \mathrm{Im}\left\{\frac{1}{s_V - M_l^2 + iM_l\Gamma_l}\right\}, \tag{C7}$$

with m_l, M_l, Γ_l being the mass of the pseudoscalar meson, mass of the vector, and width of the vector, respectively. Replacing G_{ll} with $\tilde{G}_{ll}$ in Eq. (C1), we include the width effect of vector mesons. In the present case, we only do the convolution for the ρ and K^*.

[1] R. P. Feynman, M. Gell-Mann, and G. Zweig, Group $U(6) \times U(6)$ Generated by Current Components, Phys. Rev. Lett. **13**, 678 (1964).
[2] M. Gell-Mann, A schematic model of baryons and mesons, Phys. Lett. **8**, 214 (1964).
[3] S. L. Olsen, QCD exotics, Hyperfine Interact. **229**, 7 (2014).
[4] S. Choi, Hadron and quarkonium exotica, Int. J. Mod. Phys. Conf. Ser. **31**, 1460293 (2014).
[5] J. Gasser and H. Leutwyler, Chiral perturbation theory: Expansions in the mass of the strange quark, Nucl. Phys. **B250**, 465 (1985).
[6] U.-G. Meißner, Recent developments in chiral perturbation theory, Rep. Prog. Phys. **56**, 903 (1993).
[7] V. Bernard, N. Kaiser, and U.-G. Meißner, Chiral dynamics in nucleons and nuclei, Int. J. Mod. Phys. E **04**, 193 (1995).
[8] A. Pich, Chiral perturbation theory, Rep. Prog. Phys. **58**, 563 (1995).
[9] G. Ecker, Chiral perturbation theory, Prog. Part. Nucl. Phys. **35**, 1 (1995).
[10] S. Scherer, Introduction to chiral perturbation theory, Adv. Nucl. Phys. **27**, 277 (2003).
[11] V. Bernard, Chiral perturbation theory and baryon properties, Prog. Part. Nucl. Phys. **60**, 82 (2008).
[12] H. D. Politzer and M. B. Wise, Effective field theory approach to processes involving both light and heavy fields, Phys. Lett. B **208**, 504 (1988).
[13] H. Georgi, An effective field theory for heavy quarks at low-energies, Phys. Lett. B **240**, 447 (1990).
[14] E. Epelbaum, H.-W. Hammer, and U.-G. Meissner, Modern theory of nuclear forces, Rev. Mod. Phys. **81**, 1773 (2009).
[15] J. B. Kogut, A review of the lattice gauge theory approach to quantum chromodynamics, Rev. Mod. Phys. **55**, 775 (1983).
[16] M. Luscher, S. Sint, R. Sommer, and P. Weisz, Chiral symmetry and $O(a)$ improvement in lattice QCD, Nucl. Phys. **B478**, 365 (1996).
[17] M. Luscher, S. Sint, R. Sommer, P. Weisz, and U. Wolff, Nonperturbative $O(a)$ improvement of lattice QCD, Nucl. Phys. **B491**, 323 (1997).
[18] M. A. Shifman, A. I. Vainshtein, and V. I. Zakharov, QCD and resonance physics: Sum rules, Nucl. Phys. **B147**, 385 (1979).
[19] L. J. Reinders, H. Rubinstein, and S. Yazaki, Hadron properties from QCD sum rules, Phys. Rep. **127**, 1 (1985).
[20] J. M. Dias, R. M. Albuquerque, M. Nielsen, and C. M. Zanetti, $Y(4260)$ as a mixed charmonium-tetraquark state, Phys. Rev. D **86**, 116012 (2012).
[21] D. Zhou, E. L. Cui, H. X. Chen, L. S. Geng, X. Liu, and S. L. Zhu, The D-wave heavy-light mesons from QCD sum rules, Phys. Rev. D **90**, 114035 (2014).
[22] C. D. Roberts and A. G. Williams, Dyson-Schwinger equations and their application to hadronic physics, Prog. Part. Nucl. Phys. **33**, 477 (1994).
[23] P. Maris and C. D. Roberts, Dyson-Schwinger equations: A tool for hadron physics, Int. J. Mod. Phys. E **12**, 297 (2003).
[24] C. S. Fischer, Infrared properties of QCD from Dyson-Schwinger equations, J. Phys. G **32**, R253 (2006).
[25] A. Manohar and H. Georgi, Chiral quarks and the non-relativistic quark model, Nucl. Phys. **B234**, 189 (1984).

[26] Z. Y. Zhang, Y. W. Yu, P. N. Shen, L. R. Dai, A. Faessler, and U. Straub, Hyperon nucleon interactions in a chiral $SU(3)$ quark model, Nucl. Phys. **A625**, 59 (1997).

[27] C. E. Fontoura, G. Krein, and V. E. Vizcarra, $\bar{D}N$ interaction in a color-confining chiral quark model, Phys. Rev. C **87**, 025206 (2013).

[28] J. A. Oller and E. Oset, Chiral symmetry amplitudes in the S wave isoscalar and isovector channels and the σ, $f_0(980)$, $a_0(980)$ scalar mesons, Nucl. Phys. A **620**, 438 (1997); **652**, 407(E) (1999).

[29] E. Oset and A. Ramos, Nonperturbative chiral approach to s-wave $\bar{K}N$ interactions, Nucl. Phys. **A635**, 99 (1998).

[30] J. A. Oller, E. Oset, and J. R. Pelaez, Nonperturbative Approach to Effective Chiral Lagrangians and Meson Interactions, Phys. Rev. Lett. **80**, 3452 (1998).

[31] J. A. Oller, E. Oset, and J. R. Pelaez, Meson-meson interaction in a nonperturbative chiral approach, Phys. Rev. D **59**, 074001 (1999); **60**, 099906(E) (1999); **75**, 099903(E) (2007).

[32] J. A. Oller and E. Oset, N/D description of two meson amplitudes and chiral symmetry, Phys. Rev. D **60**, 074023 (1999).

[33] J. A. Oller and U.-G. Meißner, Chiral dynamics in the presence of bound states: Kaon nucleon interactions revisited, Phys. Lett. B **500**, 263 (2001).

[34] J. Fujita and H. Miyazawa, Pion theory of three-body forces, Prog. Theor. Phys. **17**, 360 (1957).

[35] L. D. Faddeev, Scattering theory for a three particle system, Zh. Eksp. Teor. Fiz. **39**, 1459 (1960) [Sov. Phys. JETP **12**, 1014 (1961)].

[36] W. Glockle, T. S. H. Lee, and F. Coester, Relativistic effects in three-body bound states, Phys. Rev. C **33**, 709 (1986).

[37] S. Weinberg, Three-body interactions among nucleons and pions, Phys. Lett. B **295**, 114 (1992).

[38] J. M. Richard, The nonrelativistic three-body problem for baryons, Phys. Rep. **212**, 1 (1992).

[39] A. Martinez Torres, K. P. Khemchandani, and E. Oset, Three-body resonances in two-meson–one-baryon systems, Phys. Rev. C **77**, 042203 (2008).

[40] A. Martinez Torres, K. P. Khemchandani, M. Nielsen, and F. S. Navarra, Predicting the existence of a 2.9 GeV $Df_0(980)$ molecular state, Phys. Rev. D **87**, 034025 (2013).

[41] L. Roca and E. Oset, A description of the $f_2(1270)$, $\rho_3(1690)$, $f_4(2050)$, $\rho_5(2350)$ and $f_6(2510)$ resonances as multi-$\rho(770)$ states, Phys. Rev. D **82**, 054013 (2010).

[42] G. Toker, A. Gal, and J. M. Eisenberg, The Y N interactions and K^- reactions on deuterium at low-energies, Nucl. Phys. **A362**, 405 (1981).

[43] R. C. Barrett and A. Deloff, Strong interaction effects in kaonic deuterium, Phys. Rev. C **60**, 025201 (1999).

[44] A. Deloff, $\eta - d$ and $K^- - d$ zero-energy scattering: A Faddeev approach, Phys. Rev. C **61**, 024004 (2000).

[45] S. S. Kamalov, E. Oset, and A. Ramos, Chiral unitary approach to the K^- deuteron scattering length, Nucl. Phys. **A690**, 494 (2001).

[46] A. Gal, On the scattering length of the K^-d system, Int. J. Mod. Phys. A **22**, 226 (2007).

[47] J. Yamagata-Sekihara, L. Roca, and E. Oset, On the nature of the $K_2^*(1430)$, $K_3^*(1780)$, $K_4^*(2045)$, $K_5^*(2380)$ and K^*6 as K^*–multi-ρ states, Phys. Rev. D **82**, 094017 (2010); **85**, 119905(E) (2012).

[48] C. W. Xiao, M. Bayar, and E. Oset, A prediction of D^*–multi-ρ states, Phys. Rev. D **86**, 094019 (2012).

[49] R. Aaij *et al.* (LHCb Collaboration), Dalitz plot analysis of $B^0 \to \bar{D}^0\pi^+\pi^-$ decays, Phys. Rev. D **92**, 032002 (2015).

[50] M. Bayar, J. Yamagata-Sekihara, and E. Oset, The $\bar{K}NN$ system with chiral dynamics, Phys. Rev. C **84**, 015209 (2011).

[51] M. Bayar and E. Oset, Improved fixed center approximation of the Faddeev equations for the $\bar{K}NN$ system with $S = 0$, Nucl. Phys. **A883**, 57 (2012).

[52] A. Martinez Torres, K. P. Khemchandani, and E. Oset, Solution to Faddeev equations with two-body experimental amplitudes as input and application to $J^P = 1/2^+$, $S = 0$ baryon resonances, Phys. Rev. C **79**, 065207 (2009).

[53] D. Jido and Y. Kanada-En'yo, $K\bar{K}N$ molecule state with $I = 1/2$ and $J^P = 1/2^+$ studied with three-body calculation, Phys. Rev. C **78**, 035203 (2008).

[54] N. V. Shevchenko and J. Revai, Faddeev calculations of the $\bar{K}NN$ system with chirally-motivated $\bar{K}N$ interaction: I. Low-energy K^-d scattering and antikaonic deuterium, Phys. Rev. C **90**, 034003 (2014).

[55] J. Revai and N. V. Shevchenko, Faddeev calculations of the $\bar{K}NN$ system with chirally-motivated $\bar{K}N$ interaction: II. The K^-pp quasi-bound state, Phys. Rev. C **90**, 034004 (2014).

[56] K. Miyagawa and J. Haidenbauer, Precise calculation of the two-step process for $K^-d \to \pi\Sigma N$ in the $\Lambda(1405)$ resonance region, Phys. Rev. C **85**, 065201 (2012).

[57] D. Jido, E. Oset, and T. Sekihara, The $K^-d \to \pi\Sigma n$ reaction revisited, Eur. Phys. J. A **49**, 95 (2013).

[58] M. Mai, V. Baru, E. Epelbaum, and A. Rusetsky, Recoil corrections in antikaon-deuteron scattering, Phys. Rev. D **91**, 054016 (2015).

[59] M. Bayar, C. W. Xiao, T. Hyodo, A. Dote, M. Oka, and E. Oset, Energy and width of a narrow $I = 1/2$ DNN quasibound state, Phys. Rev. C **86**, 044004 (2012).

[60] K. A. Olive *et al.* (Particle Data Group), Review of Particle Physics, Chin. Phys. C, **38**, 090001 (2014).

[61] M. Bando, T. Kugo, S. Uehara, K. Yamawaki, and T. Yanagida, Is ρ Meson a Dynamical Gauge Boson of Hidden Local Symmetry? Phys. Rev. Lett. **54**, 1215 (1985).

[62] M. Bando, T. Kugo, and K. Yamawaki, Nonlinear realization and hidden local symmetries, Phys. Rep. **164**, 217 (1988).

[63] U.-G. Meißner, Low-energy hadron physics from effective chiral Lagrangians with vector mesons, Phys. Rep. **161**, 213 (1988).

[64] M. Harada and K. Yamawaki, Hidden local symmetry at loop: A new perspective of composite gauge boson and chiral phase transition, Phys. Rep. **381**, 1 (2003).

[65] R. Molina, D. Nicmorus, and E. Oset, The $\rho\rho$ interaction in the hidden gauge formalism and the $f_0(1370)$ and $f_2(1270)$ resonances, Phys. Rev. D **78**, 114018 (2008).

[66] L. Roca, E. Oset, and J. Singh, Low lying axial-vector mesons as dynamically generated resonances, Phys. Rev. D **72**, 014002 (2005).

[67] L. S. Geng, E. Oset, L. Roca, and J. A. Oller, Clues for the existence of two $K_1(1270)$ resonances, Phys. Rev. D **75**, 014017 (2007).

[68] D. Gamermann, J. Nieves, E. Oset, and E. Ruiz Arriola, Couplings in coupled channels versus wave functions: Application to the $X(3872)$ resonance, Phys. Rev. D **81**, 014029 (2010).

[69] J. Yamagata-Sekihara, J. Nieves, and E. Oset, Couplings in coupled channels versus wave functions in the case of resonances: Application to the two $\Lambda(1405)$ states, Phys. Rev. D **83**, 014003 (2011).

[70] F. Aceti and E. Oset, Wave functions of composite hadron states and relationship to couplings of scattering amplitudes for general partial waves, Phys. Rev. D **86**, 014012 (2012).

[71] J.-J. Xie, A. Martinez Torres, and E. Oset, Faddeev fixed center approximation to the $N\bar{K}K$ system and the signature of a $N^*(1920)(1/2^+)$ state, Phys. Rev. C **83**, 065207 (2011).

[72] J. Polchinski, Renormalization and effective Lagrangians, Nucl. Phys. **B231**, 269 (1984).

[73] T. Varin, D. Davesne, M. Oertel, and M. Urban, How to preserve symmetries with cut-off regularized integrals? Nucl. Phys. **A791**, 422 (2007).

[74] F. Mandl and G. Shaw, *Quantum Field Theory* (Wiley-Interscience, New York, 1984).

[75] A. Martinez Torres, E. J. Garzon, E. Oset, and L. R. Dai, Limits to the fixed center approximation to Faddeev equations: The case of the $\phi(2170)$, Phys. Rev. D **83**, 116002 (2011).

[76] J. J. Wu, R. Molina, E. Oset, and B. S. Zou, Prediction of Narrow N^* and Λ^* Resonances with Hidden Charm above 4 GeV, Phys. Rev. Lett. **105**, 232001 (2010).

[77] J. J. Wu, R. Molina, E. Oset, and B. S. Zou, Dynamically generated N^* and Λ^* resonances in the hidden charm sector around 4.3 GeV, Phys. Rev. C **84**, 015202 (2011).

[78] C. W. Xiao, M. Bayar, and E. Oset, NDK, $\bar{K}DN$ and $NDD\bar{D}$ molecules, Phys. Rev. D **84**, 034037 (2011).

[79] E. Oset, A. Ramos, and C. Bennhold, Low lying $S=-1$ excited baryons and chiral symmetry, Phys. Lett. B **527**, 99 (2002); **530**, 260(E) (2002).

[80] F. K. Guo, R. G. Ping, P. N. Shen, H. C. Chiang, and B. S. Zou, S wave $K\pi$ scattering and effects of κ in $J/\psi \to \bar{K}^{*0}(892)K^+\pi^-$, Nucl. Phys. **A773**, 78 (2006).

[81] W. Liang, C. W. Xiao, and E. Oset, Study of $\eta K\bar{K}$ and $\eta' K\bar{K}$ with the fixed center approximation to Faddeev equations, Phys. Rev. D **88**, 114024 (2013).

[82] F. K. Guo, C. Hanhart, Q. Wang, and Q. Zhao, Could the near-threshold XYZ states be simply kinematic effects? Phys. Rev. D **91**, 051504 (2015).

[83] T. Hyodo, Hadron mass scaling near the s-wave threshold, Phys. Rev. C **90**, 055208 (2014).

[84] M. Bayar, W. H. Liang, T. Uchino, and C. W. Xiao, Description of $\rho(1700)$ as a $\rho K\bar{K}$ system with the fixed center approximation, Eur. Phys. J. A **50**, 67 (2014).

[85] S. U. Chung, R. L. Eisner, S. D. Protopopescu, N. P. Samios, and R. C. Strand, Analysis of the $K\omega$ spectrum, Phys. Lett. **51B**, 413 (1974).

[86] M. Aguilar-Benitez, V. E. Barnes, D. Bassano, S. U. Chung, R. L. Eisner, E. Flaminio, J. B. Kinson, R. B. Palmer, and N. P. Samios, Production of the L Meson in the Final State $K^-p \to K^-\pi^+\pi^-p$ at 4.6 GeV/c, Phys. Rev. Lett. **25**, 54 (1970).

[87] H. R. Blieden, G. Finocchiaro, J. Kirz, C. Nef, R. Thun, D. Bowen, D. Earles, W. Faissler *et al.*, Measurement of k^{*-} production in the reaction $k^-p \to k^{*-}p$, Phys. Lett. **39B**, 668 (1972).

[88] G. D. Tikhomirov, I. A. Erofeev, O. N. Erofeeva, and V. N. Luzin, Resonances in the $K(S)K(S)K(L)$ system produced in collisions of negative pions with a carbon target at a momentum of 40 GeV, Yad. Fiz. **66**, 860 (2003) [Phys. Atom. Nucl. **66**, 828 (2003)].

[89] W. E. Cleland, A. Delfosse, P. A. Dorsaz, J. L. Gloor, M. N. Kienzle-Focacci, G. Mancarella, A. D. Martin, M. Martin *et al.*, A partial wave analysis of diffractively produced $\bar{\Lambda}p$ and $\Lambda\bar{p}$ states, Nucl. Phys. **B184**, 1 (1981).

[90] T. Armstrong *et al.* (Bari-Birmingham-CERN-Milan-Paris-Pavia Collaboration), Evidence for resonant structures in the $\Lambda\bar{p}$ system, Nucl. Phys. **227B**, 365 (1983).

[91] V. Lensky, V. Baru, J. Haidenbauer, C. Hanhart, A. E. Kudryavtsev, and U.-G. Meißner, Precision calculation of $\gamma d \to pi^+nn$ within chiral perturbation theory, Eur. Phys. J. A **26**, 107 (2005).

[92] J. Nieves and E. Ruiz Arriola, Bethe-Salpeter approach for unitarized chiral perturbation theory, Nucl. Phys. **A679**, 57 (2000).

[93] B. Borasoy, P. C. Bruns, U.-G. Meißner, and R. Nissler, A gauge invariant chiral unitary framework for kaon photo- and electroproduction on the proton, Eur. Phys. J. A **34**, 161 (2007).

[94] M. Mai, P. C. Bruns, and U.-G. Meißner, Pion photoproduction off the proton in a gauge-invariant chiral unitary framework, Phys. Rev. D **86**, 094033 (2012).

[95] M. Mai and U.-G. Meißner, Constraints on the chiral unitary $\bar{K}N$ amplitude from $\pi\Sigma K^+$ photoproduction data, Eur. Phys. J. A **51**, 30 (2015).

[96] A. Martinez Torres, K. P. Khemchandani, L. S. Geng, M. Napsuciale, and E. Oset, The $X(2175)$ as a resonant state of the $\phi K\bar{K}$ system, Phys. Rev. D **78**, 074031 (2008).

[97] K. P. Khemchandani, A. Martinez Torres, and E. Oset, The $N^*(1710)$ as a resonance in the $\pi\pi N$ system, Eur. Phys. J. A **37**, 233 (2008).

[98] M. Bayar, X. L. Ren, and E. Oset, States of $\rho D^*\bar{D}^*$ with $J=3$ within the fixed center approximation to the Faddeev equations, Eur. Phys. J. A **51**, 61 (2015).

[99] U.-G. Meißner, G. Ríos, and A. Rusetsky, Spectrum of three-body bound states in a finite volume, Phys. Rev. Lett. **114**, 091602 (2015).